Annals of Telecommunications (2020) 75:437–446
https://doi.org/10.1007/s12243-020-00756-5

FDTD propagation of VLF-LF waves in the presence of ions in the earth-ionosphere waveguide

Jean-Pierre Bérenger[1]

Received: 19 March 2019 / Accepted: 27 January 2020 / Published online: 7 February 2020

Abstract
The finite-difference time-domain (FDTD) method has been used for a long time to compute the propagation of very low frequency (VLF) and low frequency (LF) radio waves in the Earth-Ionosphere waveguide. In previously published FDTD schemes, only the electronic density of the ionosphere was accounted for, since in usual natural conditions the effect of the ion density can be neglected. In the present paper, the FDTD scheme is extended to the case where one or several ion species must be accounted for, which may occur in special natural conditions or in such artificial conditions as after high altitude nuclear bursts. The conditions that must hold for the effect of the ions not to be negligible are discussed, the FDTD scheme with ions is derived, and numerical experiments are provided to show that the effect of the ions may be significant when the ionosphere is disturbed by incident flows of γ or β rays.

Keywords Numerical method · Finite-difference · FDTD · VLF · LF · Propagation · Communication

1 Introduction

Very low frequency (VLF) and low frequency (LF) radio waves can propagate with little attenuation in the Earth-Ionosphere waveguide, permitting radio links over thousands of kilometers. To predict the propagation of such waves, the waveguide and wavehop methods were developed in years 1960–1980 [1, 2]. These methods require small computational resource, but they have drawbacks, mainly they cannot account for continuous variations of the radio path that must be composed with segments where the physical parameters are uniform.

A third method, the well-known and simpler finite-difference time-domain (FDTD) method [3], was also used for the VLF-LF propagation. The initial FDTD scheme in [4, 5] was later replaced with a more effective scheme [6]. With both [4, 6], only the electronic density is accounted for in the ionosphere. It is thus assumed that the ionic density is negligible. This is true in usual natural conditions. However, either in abnormal natural conditions [7], or in artificial conditions following high altitude nuclear bursts [8–12], intense flows of X, γ or β rays may be radiated toward the ground, which results in a significant increase of the ionic density in the Earth-Ionosphere waveguide, below altitude 100 km where the VLF-LF waves propagate. To predict the VLF-LF propagation in such conditions, the ionic density must be taken into account in the FDTD scheme.

Several FDTD schemes devoted to the propagation of electromagnetic fields through the ionosphere have been published over the years, such as [13, 14]. The present paper focuses only on the scheme [6] developed for the particular application to radio communications at VLF-LF frequencies, usually in 10–70 kHz. This scheme is extended to the case where one or several ion species are present in the lower part of the ionosphere. The governing equations with ions are derived in section 2. The physical conditions for the effect of the ions to be significant are discussed in section 3. The extended FDTD scheme is derived in section 4. Section 5 presents comparisons of FDTD solutions with known analytical solutions in the one dimensional case. Finally, section 6 shows results of calculations of VLF-LF propagation in the Earth-Ionosphere waveguide that illustrate the actual effect of artificial ionic density.

Area 1 : Transmission and communications technologies (propagation, antennas). Subject of the paper : numerical method for computing VLF-LF propagation in the Earth-Ionosphere waveguide.

✉ Jean-Pierre Bérenger
jpberenger@gmail.com

[1] Visitor at School of Electrical and Electronic Engineering, The University of Manchester, Manchester, UK

2 The governing equations in the presence of ions

Let us consider a medium with an electronic density n_e and with N species of ions, each one with ionic density n_k. We denote as m_e and e the mass and charge of the electrons, and as m_k and p_k e the masses and charges of the ions (p_k may be positive or negative). In that medium, the equations that govern the electromagnetic field (E, H), the current density of electrons J_e, and the current densities of ions J_k read

$$\mu_0 \frac{\partial \vec{H}}{\partial t} = -\vec{\nabla} \times \vec{E} \tag{1a}$$

$$\varepsilon_0 \frac{\partial \vec{E}}{\partial t} + \vec{J}_e + \sum_{k=1}^{N} \vec{J}_k = \vec{\nabla} \times \vec{H} \tag{1b}$$

$$\frac{d\vec{J}_e}{dt} + \frac{e}{m_e} \vec{J}_e \times \vec{B}_N + \upsilon_e \vec{J}_e = \epsilon_0 \omega_{pe}^2 \vec{E} \tag{1c}$$

$$\frac{d\vec{J}_k}{dt} - p_k \frac{e}{m_k} \vec{J}_k \times \vec{B}_N + \upsilon_k \vec{J}_k = \epsilon_0 \omega_{pk}^2 \vec{E} \quad (k = 1, N) \tag{1d}$$

where

$$\omega_{pe}^2 = \frac{n_e e^2}{m_e \epsilon_0} \quad ; \quad \omega_{pk}^2 = p_k^2 \frac{n_k e^2}{m_k \epsilon_0} \tag{1e}$$

Parameters ν_e and ν_k are the electron-neutral and ion-neutral collision frequencies, respectively. Vector B_N is the natural magnetic field. Quantities ω_{pe} and ω_{pk} are the plasma frequencies of the electrons and ions.

In comparison with the case where only electrons are present [4–6], N differential equations of ions (1d) are added, and the ionic current densities J_k are present in (1b). It is obvious that this would complicate the FDTD scheme, especially with the implicit scheme [6] where there would be $N+2$ unknown vectors E, J_e, J_k, ($k=1$, N) to be advanced simultaneously. This would result in more matrices than in [6]. In facts, in the region of interest for the VLF-LF radio wave propagation, which is below altitude 100 km, Eq. (1-d) can be simplified. More precisely, the term with the natural magnetic field B_N can be neglected. This results in a great simplification of the algorithm.

To show that (1d) can be simplified, let us consider its second and third terms that depend on the current density J_k. In the case where J_k and B_N are perpendicular, i.e., the case where the cross product is maximum, the two terms are equal on condition that:

$$p_k \frac{e}{m_k} \left| \vec{J}_k \right| B_0 = \upsilon_k \left| \vec{J}_k \right| \tag{2}$$

where B_0 is the modulus of B_N. The two terms are thus equal when the collision frequency $\nu_k = \nu_{k0}$, where

$$\upsilon_{k0} = p_k \frac{e}{m_k} B_0 \tag{3}$$

and the second term in (1d) is negligible if $\nu_k >> \nu_{k0}$. Assuming that the number of charges per ion $p_{ik} = 1$ and that the ions are composed with 20 nucleons, with $B_0 = 5\ 10^{-5}$ T the order of magnitude of ν_{k0} is

$$\upsilon_{k0} = \frac{1.6\ 10^{-19}}{20\ \ 1.67\ 10^{-27}} 5\ 10^{-5} \ \approx\ 250\ s^{-1} \tag{4}$$

Let us now consider the electron-neutral collision frequency in the ionosphere. Its most common profile is

$$\upsilon_e(h) = 1.82\ 10^{11}\ e^{-0.15\ h} \tag{5}$$

where h is the altitude in km. This yields ν_e(100 km) = 55,600 s^{-1}. Concerning the collision frequency of the ions, it is stated in [9] that

$$\upsilon_e/40 < \upsilon_k < \upsilon_e/10 \tag{6}$$

while other sources report a ratio ν_e/ν_k of the order of 25. Using (6), ν_k is between 1400 s^{-1} and 5600 s^{-1} at altitude 100 km, and larger below that altitude. From this, the condition $\nu_k >> \nu_{k0}$ is well verified below 100 km and especially below 90 km which is the highest altitude of reflection of the VLF-LF radio waves. Thus, the effect of the B field can be neglected in (1d) that can be replaced in FDTD calculations with

$$\frac{d\vec{J}_k}{dt} + \upsilon_k \vec{J}_k = \epsilon_0\ \omega_{pk}^2 \vec{E} \qquad (k = 1, N) \tag{7}$$

Note that applying the same reasoning as above to the equation of the electrons (1c) yields a frequency collision of about 10^7 s^{-1} for the two terms in (1c) to be equal. From (5) this is realized about altitude 70 km, in agreement with the known fact that the natural B field has no significant effect on the VLF-LF propagation below that altitude.

3 Conditions for a negligible effect of the ions

Two conditions for the effect of the ions to be negligible can be derived below altitude 70 km, where B_N term is negligible in both (1c) and (1d). Firstly, assuming there is no electron and only ion specie k, and inserting a harmonic plane wave of angular frequency ω in Maxwell Eqs. (1a)-(1b) and in (7), the following wavenumber is obtained

$$k_w^2 = \frac{\omega^2}{c^2}\left[1 - j\frac{\omega_{pk}^2}{\omega(j\omega + \upsilon_k)}\right] \tag{8}$$

From (5)–(6), $\nu_k \approx 2.5\ 10^5\ s^{-1}$ at altitude 70 km, so that below 70 km and for frequency lower than 70 kHz, $j\omega$ is at most of the order of ν_k. The order of magnitude of k_w is thus

$$k_w^2 \approx \frac{\omega^2}{c^2}\left[1 - j\frac{\omega_{pk}^2}{\omega\upsilon_k}\right] \tag{9}$$

This wavenumber reduces to the wavenumber in a vacuum $k = \omega / c$, i.e., the ions have no effect, provided that

$$n_k \ll \frac{m_k\ \varepsilon_0}{p_k^2 e^2}\omega\ \upsilon_k \tag{10}$$

With $p_k = 1$, $m_k = 20\ m_{nuc}$, where m_{nuc} is the mass of one nucleon, and $\nu_k = \nu_e/25$, condition (10) is reported in Table 1 for 20 and 60 kHz at altitudes 30, 50, 70 km.

The other condition for the ions to be negligible is that the ionic current density J_k is negligible with respect with the electronic current density J_e. With B_N neglected in (1c) and (1d), that condition can be obtained by enforcing currents in the form $J = J_0 \exp.(j\omega t)$ into (1c) and (7). Writing down the ratio of the magnitudes of the two currents yields, with $p_k = 1$

$$\frac{J_{0k}}{J_{0e}} = \frac{n_k m_e}{n_e m_k}\frac{j\omega + \upsilon_e}{j\omega + \upsilon_k} \tag{11}$$

Below 70 km, $j\omega$ is at most of the order of ν_k, and lower than ν_e. With $m_k = 20\ m_{nuc} = 36{,}700\ m_e$, and $\nu_k = \nu_e/25$, the order of magnitude of ratio (11) is thus

$$\frac{J_{0k}}{J_{0e}} \approx 7\ 10^{-4}\frac{n_k}{n_e} \tag{12}$$

from which the current of the ions is negligible with respect with the current of the electrons provided that

$$n_k \ll 1000\ \ n_e \tag{13}$$

In summary, below and about 70 km the effect of the ions is negligible provided that at least condition in Table I or condition (13) holds. Inversely, the effect of the ions may be significant if the two conditions do not hold simultaneously.

Profiles of electrons and ions (one specie) produced by flows of γ or β rays are provided in [9]. The rays propagate downward from a source assumed as situated outside the ionosphere. The source may be debris of a high altitude nuclear burst. Two nighttime profiles of electrons and positive ions from [9] are reproduced in Fig. 1, corresponding to flows of γ rays of 10^{-4} and 10^{-2} W/m^2. In [9] the ionizations are provided at altitudes 40–100 km. In Fig. 1, and in calculations, we extrapolated downward the ion density by taking account that the stopping altitude of γ rays is about 25 km in the ionosphere, which means that the ion density should decrease below 25 km. More specifically, we assumed that the densities at altitudes 35, 30, 20, 10 km equal the density at altitude 40 km multiplied with coefficients 1.05, 1.1, 0.9, 0.01, respectively.

It can be seen in Fig. 1 that at altitude 70 km $n_e \approx 10$ cm^{-3} and $n_k \approx 10^4$ cm^{-3} for $I_\gamma = 10^{-4}$ W/m^2, and that at altitude 50 km $n_e \approx 100$ cm^{-3} and $n_k \approx 3\ 10^5$ cm^{-3} for $I_\gamma = 10^{-2}$ W/m^2. In both cases, conditions (13) and in Table 1 do not hold at 20 kHz. It is thus expected a significant effect of the ions with such γ flows. This will be confirmed by numerical experiments in the following sections.

Table 1 Condition that renders the effect of ions negligible

Altitude	20 kHz	60 kHz
70 km	$n_k << 3\ 10^5$ cm^{-3}	$n_k << 9\ 10^5$ cm^{-3}
50 km	$n_k << 6\ 10^6$ cm^{-3}	$n_k << 1.8\ 10^7$ cm^{-3}
30 km	$n_k << 10^8$ cm^{-3}	$n_k << 3\ 10^8$ cm^{-3}

4 The FDTD scheme with ions

In this section we extend the implicit scheme [6] to the case where ions are present. The field and current densities are computed at the nodes of the FDTD grid in spherical coordinates, as described in [6]. In particular, the current densities are collocated in space and time with the electric field. Collocation in time permits the stability condition of the scheme to be the same as in a vacuum [6]. Here we derive FDTD schemes in the case with only one ion specie, in the case with several ion species, and finally in the special case where the natural B field can be neglected in the equation of

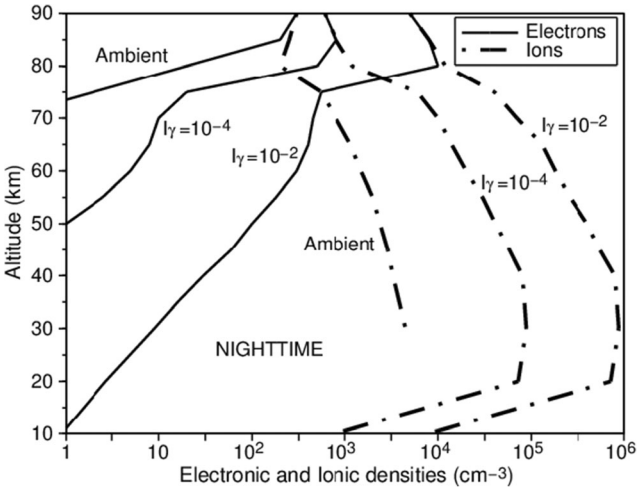

Fig. 1 Densities of electrons and ions in function of attitude in ambient ionosphere and with γ ray flows $I\gamma = 10^{-4}$ and 10^{-2} W/m^2 from [9]

electrons (1c). This special case is important in practice since it can be used below altitude 60–70 km, which results in a significant reduction of CPU time.

4.1 The FDTD scheme with one ion specie

We assume that there is only one ion specie, i.e., $N = 1$. In that case, discretization of (1b) can be expressed as

$$\overrightarrow{E}^{n+1} = \overrightarrow{E}^{n} - \frac{\Delta t}{\varepsilon_0}\frac{\overrightarrow{J}_e^{n} + \overrightarrow{J}_e^{n+1} + \overrightarrow{J}_1^{n} + \overrightarrow{J}_1^{n+1}}{2} + \frac{\Delta t}{\varepsilon_0}\overrightarrow{\nabla} \times \overrightarrow{H}^{n+1/2} \tag{14}$$

which is similar to that in [6] with just the addition of the ionic current density J_1. Concerning (1c), it is identical, rigorously, to the equation without ion, so that its discretization is the same as in [6], i.e.,

$$\overrightarrow{J}_e^{n+1} = M_1 \overrightarrow{J}_e^{n} + b_e \varepsilon_0 \omega_{pe}^2 M_2 \frac{\overrightarrow{E}^{n} + \overrightarrow{E}^{n+1}}{2} \tag{15}$$

where

$$M_1 = A_e^{-1} B_e \quad ; \quad M_2 = A_e^{-1} \tag{16a}$$

$$A_e = \frac{1}{2}\begin{pmatrix} 2 & b_e\omega_{be\phi} & -b_e\omega_{be\theta} \\ -b_e\omega_{be\phi} & 2 & b_e\omega_{ber} \\ b_e\omega_{be\theta} & -b_e\omega_{ber} & 2 \end{pmatrix}$$
$$B_e = \frac{1}{2}\begin{pmatrix} 2\,a_e & -b_e\omega_{be\phi} & b_e\omega_{be\theta} \\ b_e\omega_{be\phi} & 2\,a_e & -b_e\omega_{ber} \\ -b_e\omega_{be\theta} & b_e\omega_{ber} & 2\,a_e \end{pmatrix} \tag{16b}$$
$$\omega_{beu} = \frac{e}{m_e} B_{Nu} \quad (u = r, \theta, \phi)$$
$$a_e = e^{-\nu_e \Delta t}; \qquad b_e = \frac{1 - a_e}{\nu_e}$$

where B_{Nu} is the u component of the natural B field.

The equation of the ions (7) can be discretized as

$$\overrightarrow{J}_1^{n+1} = a_1 \overrightarrow{J}_1^{n} + b_1 \varepsilon_0 \omega_{p1}^2 \frac{\overrightarrow{E}^{n} + \overrightarrow{E}^{n+1}}{2} \tag{17}$$

where a_1 and b_1 are given by (16b) with index 1 in place of e. Eqs. (14), (15), (17), are implicit. They must be combined for providing vectors E, J_e, J_1, at time $n + 1$. Using (15) and (17) into (14) yield

$$\overrightarrow{E}^{n+1} = \overrightarrow{E}^{n} - \frac{\Delta t}{2\varepsilon_0}(I + M_1)\overrightarrow{J}_e^{n} - \frac{\Delta t}{2\varepsilon_0}(1 + a_1)\overrightarrow{J}_1^{n.}$$
$$-\frac{\Delta t}{4}\left[b_e\omega_{pe}^2 M_2 + b_1\omega_{p1}^2\right]\left(\overrightarrow{E}^{n} + \overrightarrow{E}^{n+1}\right) + \frac{\Delta t}{\varepsilon_0}\overrightarrow{\nabla} \times \overrightarrow{H}^{n+1/2} \tag{18}$$

from which the following advance of E field is obtained as

$$\overrightarrow{E}^{n+1} = W_1 \overrightarrow{E}^{n} - \frac{\Delta t}{2\,\varepsilon_0} W_2 \overrightarrow{J}_e^{n}$$
$$-\frac{\Delta t}{\varepsilon_0} W_3 \left[\frac{1 + a_1}{2}\overrightarrow{J}_1^{n} - \overrightarrow{\nabla} \times \overrightarrow{H}^{n+1/2}\right] \tag{19}$$

where matrices W_1, W_2, W_3, read

$$W_1 = W_3\left[(1-\theta_1)\, I - \theta_e M_2\right] \tag{20a}$$
$$W_2 = W_3\left[I + M_1\right] \tag{20b}$$
$$W_3 = \left[(1 + \theta_1)\, I + \theta_e M_2\right]^{-1} \tag{20c}$$

and

$$\theta_u = \frac{b_u\, \omega_{pu}^2 \Delta t}{4} \tag{20d}$$

Once E has been advanced with (19), current densities J_e and J_1 can be advanced using (15) and (17). This scheme is the extension of the implicit-1 scheme in [6]. We note that (19) requires storage of three matrices in the FDTD loop on time. With in addition M_1 and M_2 used in (15), five 3×3 matrices must be stored, as with the corresponding equation without ions [6].

The implicit-2 scheme in [6] can also be extended by using E^{n+1} from (14) into (15) that yields

$$\overrightarrow{J}_e^{n+1} = M_1 \overrightarrow{J}_e^{n} + \frac{b_e\varepsilon_0\omega_{pe}^2}{2} M_2 \left[\overrightarrow{E}^{n} + \overrightarrow{E}^{n}\right.$$
$$\left. -\frac{\Delta t}{2\,\varepsilon_0}\left(\overrightarrow{J}_e^{n} + \overrightarrow{J}_e^{n+1} + \overrightarrow{J}_1^{n} + \overrightarrow{J}_1^{n+1}\right) + \frac{\Delta t}{\varepsilon_0}\overrightarrow{\nabla} \times \overrightarrow{H}^{n+1/2}\right] \tag{21}$$

from which

$$[I + \theta_e M_2]\,\overrightarrow{J}_e^{n+1} = [M_1 - \theta_e M_2]\,\overrightarrow{J}_e^{n} - \theta_e M_2\left(\overrightarrow{J}_1^{n} + \overrightarrow{J}_1^{n+1}\right)$$
$$+4\,\theta_e M_2 \frac{\varepsilon_0}{\Delta t}\overrightarrow{E}^{n} + 2\,\theta_e M_2 \overrightarrow{\nabla} \times \overrightarrow{H}^{n+1/2} \tag{22}$$

with θ_e from (20d).

Similarly, using (14) into (17) where there is no matrix gives

$$\overrightarrow{J}_1^{n+1} = \frac{a_1 - \theta_1}{1 + \theta_1}\overrightarrow{J}_1^{n}$$
$$-\frac{\theta_1}{1 + \theta_1}\left[\left(\overrightarrow{J}_e^{n} + \overrightarrow{J}_e^{n+1} - \frac{4\varepsilon_0}{\Delta t}\overrightarrow{E}^{n} - 2\,\overrightarrow{\nabla} \times \overrightarrow{H}^{n+1/2}\right]\right. \tag{23}$$

Using J_1 from (23) into (22) yields the FDTD advance of J_e

$$\overrightarrow{J}_e^{n+1} = W_4 \overrightarrow{J}_e^{n}$$
$$+ W_5\left[-\frac{1 + a_1}{2}\overrightarrow{J}_1^{n} + \frac{2\,\varepsilon_0}{\Delta t}\overrightarrow{E}^{n} + \overrightarrow{\nabla} \times \overrightarrow{H}^{n+1/2}\right] \tag{24}$$

where matrices W_4, W_5 read

$$W_4 = \left[I + \frac{\theta_e}{1+\theta_1} M_2\right]^{-1} \left[M_1 - \frac{\theta_e}{1+\theta_1} M_2\right] \tag{25a}$$

$$W_5 = \left[I + \frac{\theta_e}{1+\theta_1} M_2\right]^{-1} 2\,\frac{\theta_e}{1+\theta_1} M_2 \tag{25b}$$

Once J_e has been advanced, J_1 can be advanced using (23), and then the E field using (14) where all the quantities in the right-hand member are known.

Comparing with the case without ions [6], we can note that (24) is in the same form as (26) in [6] with just an additional term with the ionic current J_1. There are two matrices, W_4 and W_5 in (24), so that the presence of one specie of ions lets unchanged the number of matrices to be stored in the FDTD loop on time since two out of the three matrices in (26) of [6] just differ with a scalar parameter. The ions require the addition of the J_1 term in (14), and obviously the advance of the ionic current using (23) where there is no matrix. At the end, taking account of one ion specie left about unchanged the memory requirements (no additional matrix).

The implicit-2 scheme (14), (23), (24). relies on only one equation involving two matrices (24), while the implicit-1 scheme relies on two equations, (15) and (19), involving five matrices. The implicit-2 scheme is thus more effective in terms of needed memory and CPU time, as without ions [6].

4.2 The FDTD scheme with several ion species

Let us now address the case where there are several ion species. The implicit-1 scheme in previous section can be easily extended. Eq. (14) is replaced with

$$\vec{E}^{n+1} = \vec{E}^{n} - \frac{\Delta t}{2\,\varepsilon_0}\left[\vec{J}_e^{\,n} + \vec{J}_e^{\,n+1} + \sum_{k=1}^{N}\left(\vec{J}_k^{\,n} + \vec{J}_k^{\,n+1}\right)\right]$$

$$+ \frac{\Delta t}{\varepsilon_0}\vec{\nabla} \times \vec{H}^{n+1/2} \tag{26}$$

and we have a set of N equations similar to (17) for the N ion species. Enforcing them and (15) into (26), we obtain, in place of (18)

$$\vec{E}^{n+1} = \vec{E}^{n} - \frac{\Delta t}{2\varepsilon_0}(I + M_1)\vec{J}_e^{\,n} - \frac{\Delta t}{2\varepsilon_0}\sum_{k=1}^{N}(1+a_k)\vec{J}_k^{\,n}$$

$$- \frac{\Delta t}{4}\left[b_e\omega_{pe}^2 M_2 + \sum_{k=1}^{N} b_k\omega_{pk}^2\right]\left(\vec{E}^{n} + \vec{E}^{n+1}\right)$$

$$+ \frac{\Delta t}{\varepsilon_0}\vec{\nabla} \times \vec{H}^{n+1/2}$$

from which

$$\vec{E}^{n+1} = W_6\vec{E}^{n} - \frac{\Delta t}{2\,\varepsilon_0} W_7\vec{J}_e^{\,n}$$

$$- \frac{\Delta t}{\varepsilon_0} W_8\left[\sum_{k=1}^{N}\frac{1+a_k}{2}\vec{J}_k^{\,n} - \vec{\nabla} \times \vec{H}^{n+1/2}\right] \tag{27}$$

where

$$W_6 = W_8\left[\left(1 - \sum_{k=1}^{N}\theta_k\right) I - \theta_e M_2\right] \tag{28a}$$

$$W_7 = W_8\left[I + M_1\right] \tag{28b}$$

$$W_8 = \left[\left(1 + \sum_{k=1}^{N}\theta_k\right) I + \theta_e M_2\right]^{-1} \tag{28c}$$

Once E has been advanced, J_e can be advanced with (15) and the N ion currents J_k with their own equations like (17). We note that the number of matrices to be stored in the loop on time remains the same as without ions, that is M_1, M_2, W_6, W_7, W_8. Concerning the computational time, adding more ion species mainly adds more Eq. (17) where there is no matrix.

Extending the implicit-2 scheme to several ion species is possible by replacing E^{n+1} from (26) into (15) and in Eq. (17) of each specie. A set of $N+1$ equations is obtained for the $N+1$ unknown currents J_e^{n+1} and J_k^{n+1}. We solved the set for $N=2$. More generally, it can be seen that for any N, the advance of J_e^{n+1} involves only two matrices, as (24), and the advances of the J_k^{n+1} remain scalar equations, as (23). However, these N scalar equations involve all the J_k^n currents and are thus more time consuming than the N Eq. (17) of the advances of the implicit-1 currents. So that the implicit-2 scheme would become less effective in terms of CPU time for N large enough. For this reason, and because it is more complex, we have not further investigated the implicit-2 scheme.

4.3 The special case where the natural *B* field is negligible

Let us write down the equations of the advance of the E field and J current densities in the case where the natural B field has no effect for both ions and electrons. This occurs below 60–70 km in altitude and can significantly reduce the computational time by using simplified equations. In that case, the B field term is absent in (1c), as in the ion Eq. (7). With N ion species, Eq. (27) of the implicit-1 scheme reduces to

$$\vec{E}^{n+1} = \frac{1-\theta_e-\sum_{k=1}^{N}\theta_k}{D}\vec{E}^{n} - \frac{\Delta t}{2\,\varepsilon_0 D}(1+a_e)\vec{J}_e^{n} - \frac{\Delta t}{2\,\varepsilon_0 D}\sum_{k=1}^{N}(1+a_k)\vec{J}_k^{n} + \frac{\Delta t}{\varepsilon_0 D}\vec{\nabla}\times\vec{H}^{n+1/2} \quad (30)$$

with θ_e and θ_k from (20d) and $D = 1 + \theta_e + \sum_{k=1}^{N}\theta_k$. Then the $N+1$ currents J_e and J_k can be advanced with equations like (17). It can be seen that because of the absence of matrices, this implicit-1 scheme is more effective than the corresponding implicit-2 scheme with any number of ion species.

5 Numerical experiments in one dimension

We performed comparisons of the theoretical propagation with the FDTD propagation in the simple one dimensional case where there is no natural B field, with the objective of validating the above described FDTD schemes in the presence of ions and to illustrate the fact that the ions cannot be neglected in some unusual Ionospheric conditions.

The experiments were performed with electronic and ionic profiles from [9] produced by γ ray flows (two profiles are reproduced in Fig. 1). Below altitude 100 km, there are numerous ion species. The most important are O_2^+, NO^+, O^+, N^+. In [9], and consequently in Fig. 1, the species are not detailed, the ionic density is the total density. We thus mainly performed calculations with one ion specie, with mass of ions assumed as 20 masses m_{nuc} of one nucleon, and with positive charge of ions equal to that of one electron. The collision frequency of the ions was $\nu_k(h) = \nu_e(h)/25$ with $\nu_e(h)$ from (5).

In the absence of B field and with electrons and N ion species, the equation of dispersion in the medium reads

$$k_w^2 = \frac{\omega^2}{c^2}\left[1 - j\frac{1}{\omega}\left(\frac{\omega_{Pe}^2}{j\omega+\upsilon_e} + \sum_{k=1}^{N}\frac{\omega_{Pk}^2}{j\omega+\upsilon_k}\right)\right] \quad (31)$$

where k_w is the wavenumber. By expressing it in km^{-1}, the incremental attenuation of a wave propagating in the medium is then

$$A_{th}\,(dB/km) = -20\,log\left[e^{imag(k_w)}\right] \quad (32)$$

FDTD calculations were performed within a 1D domain filled with a uniform medium, with a Gaussian source impressed at the left-hand boundary. The field E_{obs} was observed 10 km from the source. The domain was large enough not to see the reflection from the right-hand boundary. The incremental attenuation at frequency f was computed as

$$A_{FDTD}\,(dB/km) = -20\,log\left(\frac{E_{obs}(f)}{E_s(f)}\right)/10 \quad (33)$$

where $E_s(f)$ and $E_{obs}(f)$ are the Fourier transforms of the Gaussian source and of the observed field, respectively. For every considered ionosphere, the FDTD simulation was performed several times with homogeneous media corresponding to a set of altitudes separated with 5 km. The FDTD space step was 500 m.

Fig. 2 compares the theoretical attenuation (32) with the FDTD attenuation (33) in function of altitude, for frequency 20 kHz and a daytime ionosphere struck by γ flow $I_\gamma = 10^{-4}$ W/m^2 in [9]. Three attenuations were computed and plotted, with electrons only, with ions only, and with both electrons and ions. As can be seen, the effect of the ions is not negligible. Below 45 km the attenuation of the ions is preponderant. Fig. 3 is similar to Fig. 2, with same I_γ, but during nighttime (profile in Fig. 1). The effect of the ions is larger than during daytime, with a ionic absorption widely larger than the electronic absorption up to about 60 km. In Fig. 4, the γ flow is larger, $I_\gamma = 10^{-2}$ W/m^2. Again, the effect of ions is important, here it is preponderant below altitude 50 km.

We note that FDTD attenuations (33) in Figs. 2, 3, and 4 closely agree with the theoretical absorption computed using (31). FDTD calculations were performed with implicit-1 scheme (15), (17), (19), and with implicit-2 scheme (14), (23), (24). They yield same results (indistinguishable in figures). These results thus validate the implicit FDTD schemes in the presence of ions, at least without B field.

The incremental attenuations may appear as small in Figs. 2, 3, and 4. To predict the effect on VLF-LF propagation in the Earth-Ionosphere waveguide, we must consider that the radio wave traverses at least two times the absorbing region with an elevation angle (angle formed by the path and the ground) which is typically in 0–20°. To provide us with an order of magnitude of the attenuation experienced by a

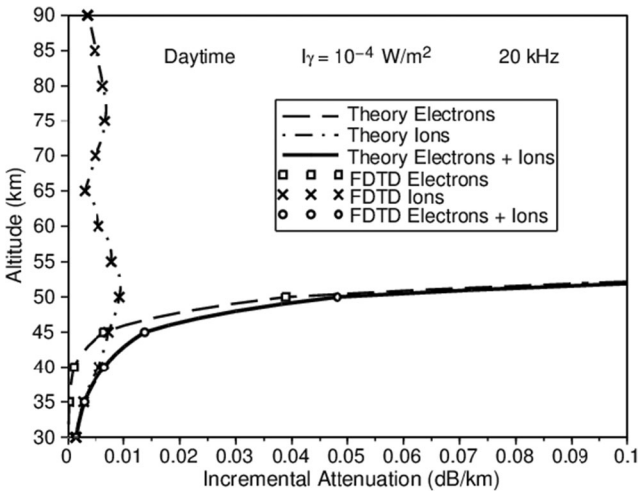

Fig. 2 Comparison of theoretical attenuation (32) with FDTD attenuation (33), for electrons, ions, and both electrons and ions, produced during daytime by a γ flow $I_\gamma = 10^{-4}$ W/m^2

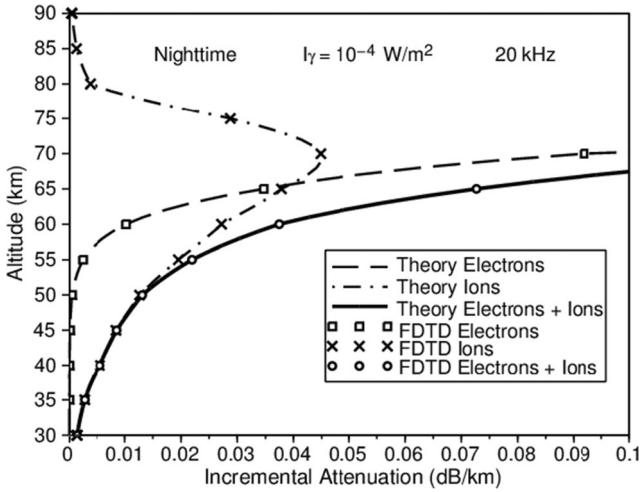

Fig. 3 Comparison of theoretical attenuation (32) with FDTD attenuation (33), for electrons, ions, and both electrons and ions, produced at night by a γ flow $I_\gamma = 10^{-4}$ W/m^2

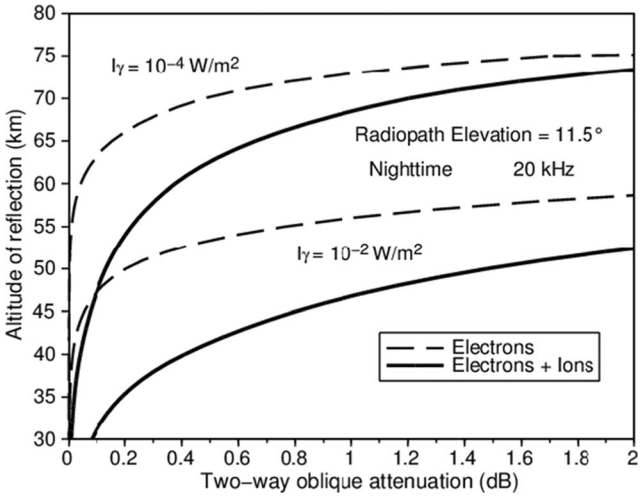

Fig. 5 Two-crossing attenuation with γ flows 10^{-4} and 10^{-2} W/m^2 for a 20-kHz oblique radiopath of elevation angle 11.5°

realistic VLF radiopath, the attenuation for a two-crossing radiopath between the ground and a given altitude is plotted in Fig. 5, for elevation angle 11.5° and γ flows in Figs. 3 and 4. Results in Fig. 5 are thus the integrals of the incremental absorptions in Figs. 3 and 4, multiplied with 10 (factors of 2 for two-crossing, and 5 since cos (11.5°) = 0.2). With Fig. 5 we cannot predict the experienced attenuation in an exact manner, since it depends on the altitude of reflection, but we can see that the attenuation due to the ions may be significant, at least of the order of one dB, or more for long range radiopaths with several hops. This will be confirmed in next section

The impicit-1 scheme was also tested with several ion species, again in the absence of B field where the E field is advanced using (30). Some results are reported in Fig. 6.

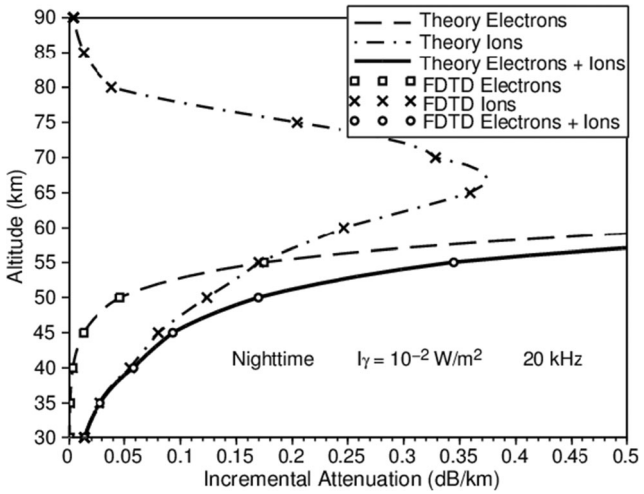

Fig. 4 Comparison of theoretical attenuation (32) with FDTD attenuation (33), for electrons, ions, and both electrons and ions, produced at night by a γ flow $I_\gamma = 10^{-2}$ W/m^2

Electrons and ion specie 1 are the $I_\gamma = 10^{-4}$ W/m^2 profiles, as in Fig. 3, ion specie 2 is the nighttime ion profile of $I_\gamma = 10^{-2}$ W/m^2, and ion specie 3 is the daytime ion profile of $I_\gamma = 10^{-2}$ W/m^2. The masses of the three species were $m_1 = 20\ m_{nuc}$, $m_2 = 60\ m_{nuc}$, $m_3 = 16\ m_{nu}$. As can be observed, the FDTD attenuations computed with imlicit-1 scheme (17), (30), are in close agreement with the theoretical attenuations (32).

6 Propagation of VLF-LF waves in the earth-ionosphere waveguide

This section compares the VLF and LF propagation with and without positive ions in the Earth-Ionosphere waveguide

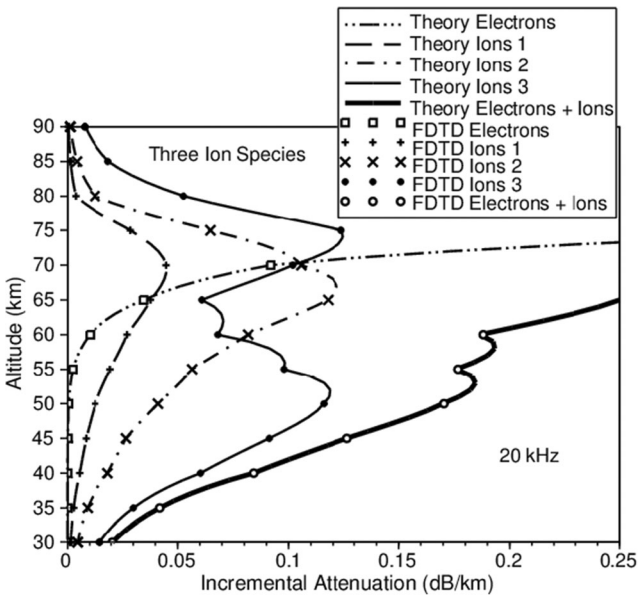

Fig. 6 Comparison of theoretical attenuation (32) with FDTD attenuation (33) produced by electrons and three ion species at frequency 20 kHz

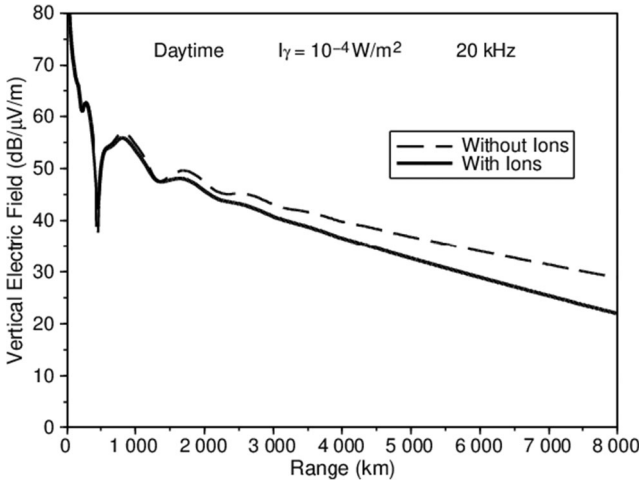

Fig. 7 Comparison of VLF signals (20 kHz) computed with and without ions for a daytime γ flow $I_\gamma = 10^{-4}$ W/m^2

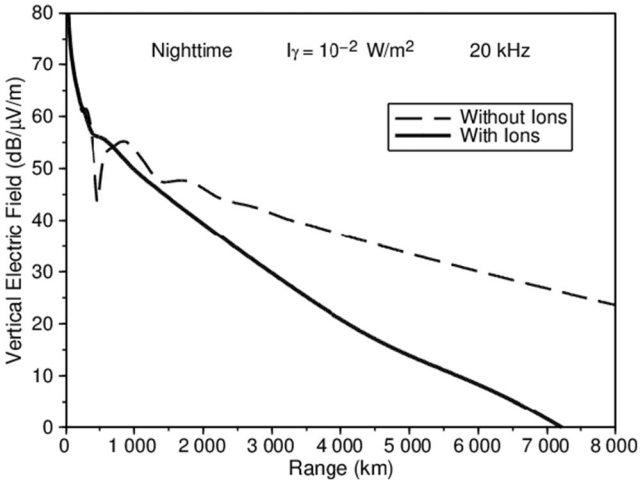

Fig. 9 Comparison of VLF signals (20 kHz) computed with and without ions for a nighttime γ flow $I_\gamma = 10^{-2}$ W/m^2

disturbed by artificial flows of γ or β rays [9]. Since only the total ionic density is provided in [9], it was assumed that there is only one ion specie in the ionosphere. The calculations were performed with the CODIF computer code [4, 5] whose current version relies on the FDTD scheme [6]. It is a two dimensional (2D) code, in spherical coordinates (r, θ, $\varphi = 0$), with part of the computational domain where the plasma is anisotropic, due to the natural magnetic field that has a significant effect on the VLF-LF propagation during nighttime. The one-ion-specie implicit-1 scheme (15), (17), (19), and implicit-2 scheme (14), (23), (24), were implemented and compared. They yield same results (indistinguishable in figures). The implicit-2 scheme has been retained as the default scheme since it is less demanding in computational resource. It is used at altitudes where the natural B field cannot be neglected in the equations of the electrons (1c). At low altitudes where the term with B_N can be neglected in (1c), the simplified implicit-1 scheme (30) is used to reduce the computational requirements. The transition between the two schemes was at attitude 70 km in the reported calculations (70 km is the default transition retained after experiments).

In the calculations, the mass of the ions was assumed as 20 times the mass of one nucleon, the ion-neutral collision frequency was (5) divided with 25, the B field was oriented 45° from the ground and 45° from the plane of propagation, with magnitude 5 10^{-5} T. The transmitter was a vertical dipole radiating 1 kW, and the Earth ground was assumed as a perfect conductor. The FDTD steps were 1 km and 333 m for transmitter frequencies 20 and 60 kHz.

Fig. 7 shows the vertical E field on the ground as a function of distance from a 20-kHz transmitter, computed with and without ions, for a daytime ionosphere disturbed by a γ flow $I_\gamma = 10^{-4}$ W/m^2. Fig. 8 shows the same comparison, but during nighttime. Fig. 9 is similar to Fig. 8, but with $I_\gamma = 10^{-2}$ W/m^2. In all the cases the ions have a significant effect on the signal strength. In Figs. 8 and 9 the ions reduce the signal by

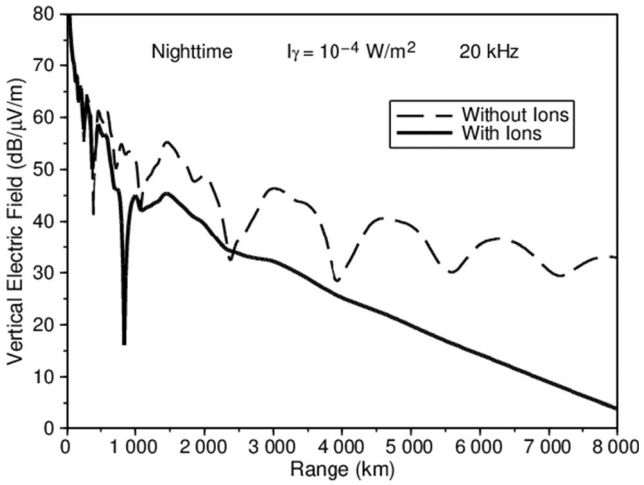

Fig. 8 Comparison of VLF signals (20 kHz) computed with and without ions for a nighttime γ flow $I_\gamma = 10^{-4}$ W/m^2

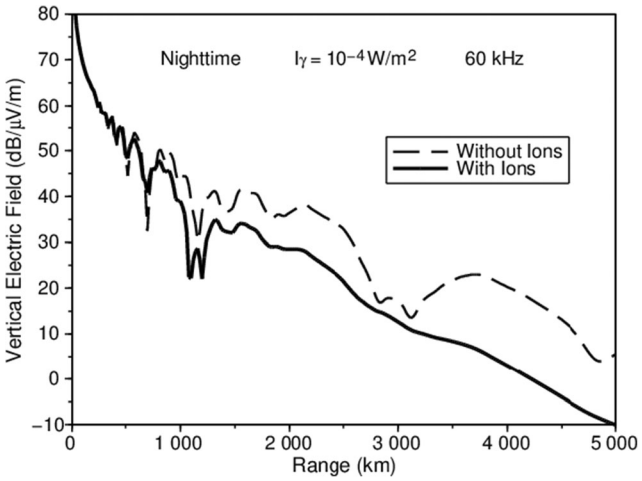

Fig. 10 Comparison of LF signals (60 kHz) computed with and without ions for a nighttime γ flow $I_\gamma = 10^{-4}$ W/m^2

about 20 dB at the end of the 8000-km radio path. This is quite large since in natural conditions VLF signals decrease slowly with distance, typically by 2–3 dB/1000 km. Interpretation of results in Figs. 7, 8, and 9 using incremental attenuations in Figs. 2, 3, and 4 is not easy since the VLF signal attenuation depends on several parameters (elevation angles of the preponderant modes, altitudes of reflection, number of hops) that are modified when the ionosphere is disturbed. However, the attenuation by ions in Fig. 8 appears as consistent with Figs. 3 and 5, while the attenuation in Fig. 7, during daytime, is smaller than in Fig. 8, which is also consistent with the smaller attenuation in Fig. 2 than in Fig. 3.

Calculations were also performed with larger γ flows [9]. The effect of the ions decreases when I_γ grows, in accordance with the decrease of the ratio n_i/n_e [9] at low altitudes which implies that condition (13) becomes true.

Fig. 10 is a comparison with/without ions at LF frequency 60 kHz. Again, the signal is widely reduced by the γ flow $I_\gamma = 10^{-4}$ W/m^2. Finally, Fig. 11 shows the effect of ions with the ionosphere disturbed by a β flow $N_\beta = 10^4$ cm^{-2} s^{-1} from [9]. The attenuation due to the ions is rather smaller than that observed with the γ rays, which is not surprising since the modifications of the ionosphere by γ and β rays are different because the stopping altitude of β rays is about 55 km instead of 25 km.

In summary, with the artificial disturbances of the ionosphere in [9], the effect of the ions on VLF and LF propagation may widely reduce the signal strength at long distance from the transmitter, resulting in a large reduction of the actual radio link lengths**.** Notice that the reduction of the signal weakly depends on the mass of ions used in the calculations. As an example, the signal 8000 km from the transmitter differs with about 3 dB in Figs. 8 and 9 by using a mass of ions of 25 mass of one nucleon in place of 20.

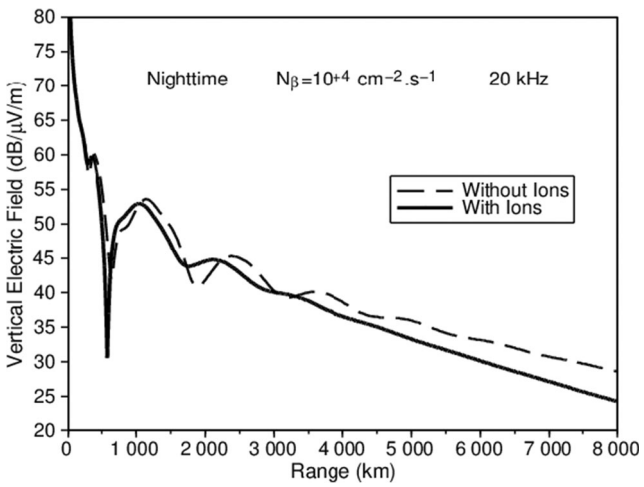

Fig. 11 Comparison of VLF signals (20 kHz) computed with and without ions for a nighttime β flow $N_\beta = 10^4$ cm^{-2}.s^{-1}

Concerning the computational time of the computer code, with ions it is increased by about 50% as compared to the same calculation without ions. The computational times of simulations thus remain of the order of 1 min at VLF and 10 min at LF using a single thread on a personal computer. They can be easily reduced by a factor about 5 by using Open MP parallelization and a 8-thread computer.

7 Conclusion

The FDTD scheme used to compute the propagation of VLF-LF radio waves in the Earth-Ionosphere waveguide [6] has been extended so as to be able to account for the presence of ions in the ionosphere. This permits the computer code relying on the FDTD method to deal with any disturbance of the ionosphere, either a natural disturbance [7] or such an artificial disturbance as a nuclear event [8].

Taking account of the physical parameters of the VLF-LF radio link problem, namely the frequency usually in 10–70 kHz, the altitude of reflection lower than 100 km, and the ion-neutral collision frequency at those altitudes, the auxiliary equation governing the ions has been simplified with the objective of reducing as much as possible the additional computational requirements due to the ions. The modification of the FDTD scheme thus results in a relatively small increase of the computational requirements, and consequently preserves the possibility of using the computer code on a personal computer, even when numerous radio links are of interest.

References

1. Budden KG (1985) The propagation of radio waves. Cambridge University Press, Cambridge
2. Wait JR (1970) Electromagnetic waves in stratified media. Pergamon Press, Oxford
3. Taflove A, Hagness S (2000) Compuational electrodynamics. The finite-difference time-domain method. Artech House
4. Thévenot M, Bérenger J-P, Monedière T, Jecko F (1999) A FDTD scheme for the computation of VLF-LF propagation in the anisotropic earth-ionosphere waveguide. Ann Telecommmun 54:297–310
5. Bérenger J-P (2002) FDTD computation of VLF-LF propagation in the earth-ionosphere waveguide. Ann Telecommun 57:1059–1090
6. Bérenger J-P (2014) An implicit FDTD scheme for the propagation of VLF-LF radio waves in the earth-ionosphere waveguide. C R Physique 15:393–402
7. Sulic DM, Sreckovic VA, Mihajlov AA (2016) A study of VLF-LF signal variations associated with the changes of ionization level in the D-region in consequence of solar conditions. Adv Space Res 57:1029–1043
8. Keppler E, Pfotzer G, Riedler W (1964) Radioactive debris from nuclear explosions in high altitudes. J Atmos Terr Phys 26:429–436

9. Knapp W, Schwartz K (1975) Aids for the study of electromagnetic blackout. General Electric Company. http://www.dtic.mil/dtic/tr/fulltext/u2/a010228.pdf
10. Crain CM (1975) An overview discussion of propagation effects of nuclear environments on VLF-LF communications systems. The Rand Corporation. www.dtic.mil/dtic/tr/fulltext/u2/a024956.pdf
11. Field E (1975) VLF-LF TE-mode propagation under disturbed ionosphere conditions. Pacific Sierra Research Corporation. www.dtic.mil/dtic/tr /fulltext/u2/a016527.pdf
12. Knapp W (1979) Summary of communication and navigation systems degradation in a nuclear environment. General Electric Company. http://www.dtic.mil/dtic/tr/fulltext/u2/a196802.pdf
13. Hu WH, Cummer SA (2006) An FDTD model for low and high altitude lightning-generated EM fields. IEEE Trans Antennas Propag 54:1513–1522
14. Yu Y, Simpson J (2010) An E-J collocated 3-D FDTD model of electromagnetic wave propagation in magnetized cold plasma. IEEE Trans Antennas Propag 58:469–479